Journal of Global Environment Engineering, Vol. 12, pp.13-32, 2007

INTEGRATED MODEL FOR ESTIMATING SEDIMENT DISCHARGE TO COASTAL AREA FROM RIVER BASIN --*A CASE STUDY OF SAKAWA RIVER*

Joel NOBERT[1] *and Tomoya SHIBAYAMA*[2]

Abstract

In this study an integrated model to estimate total sediment discharge from a river basin to coastal area is proposed. The model consists of soil erosion estimation and transport mechanism components and one-dimensional river profile change component. Sakawa river basin that has an area of approximately 570 km^2 is selected as a case study. The basin boundary is delineated from the Digital Elevation Model (DEM) data using GIS software. The input parameters for the model were derived from rainfall data, land use/ land cover data, soil data and elevation data. The average annual sediment discharge to the river mouth is estimated to be about 6.7×10^4 ton/yr. The simulated sediment discharge at the river mouth is also compared with the measured sediment at the river mouth and the results show reasonably good fit. Also the effect of land use and climate change to the sediment yield is analyzed. The land use data derived from remotely sensed images of 1976 and 1997 is used as the basis for comparison to see the effect of land use change. It was observed that using the land use data for the year 1997, total sediment discharge to the coastal environment increased as compared to the year 1976; this is mainly due to the increased agricultural areas and residential areas and also decreases in forest area. For analyzing the effect of climate change, HadCM2 model is used to generate mean daily precipitation for the month for the period 2040-2050 and then daily rainfall amount is generated from this data using exponential distribution. The results of the sediments discharge to the coastal environment using this generated data show a decrease in the average annual sediment discharge.

Keywords: integrated model, land use change, climate change

1. Introduction

Watershed sediment yield is a direct indication of surface erosion rates and is also the primary source of sediment discharge to the river mouths. Hydrologic processes of rainfall and runoff drive the surface erosion process. Surface erosion by water embodies the process of detachment, transportation, and deposition of soil particles by the erosive and transport agents of raindrop impact and runoff over soil surface. Detachment and deposition is caused by the interplay between the shear stress exerted by water on the loose soil bed and the tendency of soil particles to settle under the force of gravity (Woolhiser *et al.*, 1990). The soil detachment/deposition rate is proportional to the difference between the sediment transport capacity and the sediment load in the flow.

[1] Lecturer, Water Resources Engineering Department, University of Dar es Salaam, P.O Box 35131, Dar es Salaam Tanzania; Tel/Fax: +255-22-241-0029; E-mail: nobert@wrep.udsm.ac.tz

[2] Professor, Civil Engineering Department, Yokohama National University, 79-5 Tokiwadai Hodogaya-ku, Yokohama 240-8501, JAPAN; Tel: +81-45-339-4036, Fax: +81-45-348-4565 E-mail: tomo@ynu.ac.jp

Erosion not only reduces productivity of cropland but may also degrade water quality because of the association of pollutants to the fine sediments. Deposition in water conveyance structures such as irrigation canals, stream channels, reservoir, estuaries, and harbors reduces the capacity of these structures (Foster, 1982). Despite recognition of the imposing hindrance of soil erosion, measurement is rare to absent, because it is often time consuming and data on soil erosion are limited to few sites (Lu *et al.*, 2001). This data is necessary for land management decisions in assigning priorities for erosion control (Moore and Burch, 1986). Assessment and mitigation of sediment input is a major issue for the sustainable management of coastal zones and soil erosion caused by rainfall and runoff is of particular concern.

Erosion on land surfaces has been experimentally studied by many researchers in the laboratories and in the field (Govindaraju and Kavvas, 1992). However, they have practical disadvantages that limit their application. They are expensive, time consuming and generate point-based data, which in strict sense may be valid for only the plot location. Also many mathematical models have been developed to estimate sediment yield from the watershed, but most of these models consider sediment transport in terms of sediment delivery ratio. Recently, some physically based numerical models are developed to simulate erosion and transport of sediment, e.g., Tayfur (2004); his model is based on experimental plot. In this study an integrated model which includes the effect of river profile change component is proposed.

2. Methodology

2.1 Subbasin delineation

Using the digital elevation data for the Sakawa river basin with spatial resolution of 50 m × 50 m, the basin is divided into 19 subbasins as shown in Figure 1 using ArcView GIS software. Soil erosion calculation was then performed for each subbasin. The area of the basin is 571.6 km^2 and the river originates from Fuji, Tanzawa and Hakone mountains. The river system has several branches, which include Yotsuke, Kawachi, Koyamasano and Kari rivers.

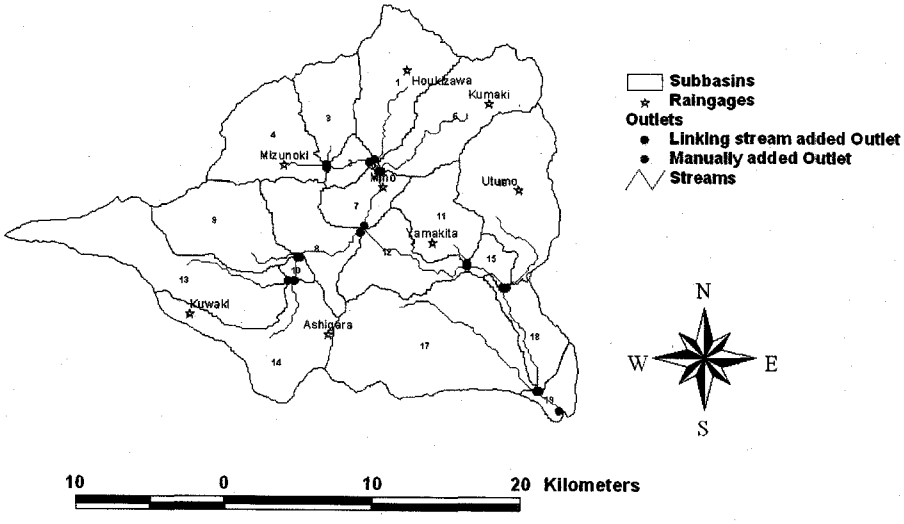

Figure 1. Subbasins in Sakawa river basin delineated from Digital Elevation Data.

2.2 Soil erosion equations

In this study, the Modified Universal Soil Loss Equation (MUSLE), (Williams, 1975, 1985) is used to estimate soil erosion caused by rainfall and runoff:

$$sed = 11.8(Q_{surf} \times q_{peak} \times area_{hru})^{0.56} \times K_{USLE} \times C_{USLE} \times P_{USLE} \times LS_{USLE} \quad (1)$$

where *sed* is the sediment yield on a given day [tons], Q_{surf} is the surface runoff volume [mm/ha], q_{peak} is the peak runoff rate [m^3/s], K_{USLE} is the soil erodibility factor [ton·m^2·hr/ (m^3·ton·cm)], $area_{hru}$ is the area of the sub-basin [ha], LS_{USLE} is the slope length factor [m] and C_{USLE} and P_{USLE} are land cover and land management factors respectively [-].

(1) Runoff volume (Q_{surf})

The runoff volume Q_{surf} is estimated using Soil Conservation Service (SCS) curve number equation (SCS, 1972)

$$Q_{surf} = \frac{(R_{day} - I_a)^2}{(R_{day} - I_a + S)} \quad (2)$$

where I_a is the initial abstractions which includes surface storage, interception and infiltration prior to runoff [mm], R_{day} is the daily rainfall [mm] and S is the retention parameter [mm].

The retention parameter varies spatially due to changes in soils, land use, management and slope and temporarily due to changes in soil water content. The retention parameter is defined as:

$$S = 25.4\left(\frac{1000}{CN} - 10\right) \quad (3)$$

where CN is the curve number; it represent the potential for storm water runoff in the drainage area.

(2) Peak runoff rate (q_{peak})

Peak runoff rate is calculated with a modified rational equation (USDA-SCS 1986):

$$q_{peak} = \frac{\alpha \times q \times A}{3.6 t_c} \quad (4)$$

where q_{peak} is the peak runoff rate [m^3/s], q is runoff [mm]; A is subbasin area [km2], t_c is time to concentration [hr] and α is the dimensionless parameter [-] that expresses the proportion of total rainfall that occurs during t_c.

The time of concentration can be calculated as a sum of overland flow time (the longest time needed for the overland flow to reach the channel) and the channel flow time (the longest time it takes water to travel from the upland channels to the outlet). The overland time of concentration can be calculated as (Arnold et al., 1995):

$$t_{ov} = \frac{L^{0.6} \times n^{0.6}}{18 \times S^{0.3}} \quad (5)$$

where t_{ov} is the overland time of concentration [hr], L is the slope length [m], n is the Manning's roughness coefficient for overland flow, and S is the slope steepness [m/m].

The channel time of concentration is calculated as:

$$t_{ch} = \frac{0.62 \times L_c \times n^{0.75}}{A^{0.125} \times S_{ch}^{\ 0.375}} \tag{6}$$

where t_{ch} is the channel time of concentration [hr], Lc is the channel length from the most distant point to the watershed outlet [km], n is the Manning's roughness coefficient, and S_{ch} is the channel slope [m/m].

(3) Soil erodibility: K_{USLE} factor

The method used for estimating the soil erodibility factor is that used in the EPIC model (Sharpley and Williams, 1990).

$$K = \frac{1}{7.6}\left\{0.2 + 0.3\exp\left[-0.0256SAN\left(1 - \frac{SIL}{100}\right)\right]\right\}\left(\frac{SIL}{CLA + SIL}\right)^{0.3} \left(1.0 - \frac{0.25OM}{orgC + \exp(3.72 - 2.95OM)}\right)\left(1.0 - \frac{0.7SN}{SN + \exp(-5.51 + 22.9SN)}\right) \tag{7}$$

where $SN = 1.0 - SAN/100$ and SAN, *SIL, CLA and OM* are the percentage content of sand, silt, clay and organic matter respectively [%].

(4) The Slope length and steepness factor: LS factor

The factor is calculated using the following equation:

$$LS = \left(\frac{L}{22.1}\right)^m \left(65.41\sin^2\theta + 4.56\sin\theta + 0.065\right) \tag{8}$$

where L is the slope length [m], m is the exponential term [-], and θ is the angle of the slope [deg.].

The exponential term, m is calculated as follows:

$$m = \left(\frac{F}{1+F}\right) \text{ and } F = \left(\frac{\sin\theta / 0.0896}{3(\sin\theta)^{0.8} + 0.56}\right) \tag{9}$$

2.3 River profile change model

2.3.1 Flow equation

One-dimensional steady flow, momentum equation is used for the flow calculation:

$$\frac{\partial H}{\partial x}+\frac{\partial}{\partial x}\left(\frac{\psi Q^2}{2gA^2}\right)+i_e=0 \tag{10}$$

$$i_e=\frac{u^2n^2}{R^{4/3}} \tag{11}$$

where x is the distance from the river mouth [m], H is the water surface elevation [m], Q is the river discharge [m^3/s], A is the cross-section area [m^2], R is the hydraulic radius [m], i_e is the energy slope, ψ is the energy correction coefficient [-] and n is the Manning's coefficient [$s/m^{1/3}$].

Substituting Equation (11) into Equation (10), assuming $\psi = 1$ and $R = h$; Equation (10) can be re-written as:

$$\frac{\partial H}{\partial x}+\frac{Q^2}{2g}\frac{\partial}{\partial x}\left(\frac{1}{B^2h^2}\right)+\frac{Q^2n^2}{B^2h^{10/3}}=0 \tag{12}$$

$$H=\eta+h \tag{13}$$

where η is the river is bed elevation [m], B is the width of the river [m] and h is the water depth [m].

2.3.2 Sediment equations

(i) Bed load equations

The bed load transport rate per unit width is calculated by Ashida and Michiue's formula (1972):

$$\frac{q_{Bi}}{\sqrt{sgd_i^3}}=p_i 17\gamma_{*i}^{'3/2}\left(1-\frac{\gamma_{*ci}}{\gamma_{*i}}\right)\left(1-\frac{u_{*ci}}{u_*}\right) \tag{14}$$

$$\frac{u_{*ci}^{\ 2}}{u_{*cm}^{\ 2}}=\left[\frac{\log 23}{\log\left(21\frac{d_i}{d_m}+2\right)}\right]\frac{d_i}{d_m} \tag{15}$$

where q_{Bi} is the bed load [m^3/s] per unit width, d_i the diameter of the bed material [m], P_i is the volumetric fraction of the sediment particles [-], S is the specific gravity of the sediment particles [-], γ_{*i} is the non-dimensional shear stress [-], γ_{*ci} is the non-dimensional critical shear stress [-], and u_{*ci} is the critical shear velocity [m/s].

(ii) Suspended load equations

The pick-up rate of the suspended load per unit area is calculated by the formula of Itakura and Kishi (1980).

$$q_{sui} = p_i K\left(\alpha_* \frac{\rho_s - \rho}{\rho_s} \frac{g d_i}{u_*'} \Omega_i - w_{fi} \right) \tag{16}$$

$$\Omega_i = \frac{\gamma_{*i}'}{B_{*i}} \frac{\int_{a'}^{\infty} \xi \frac{1}{\sqrt{\pi}} \exp(-\xi^2) d\xi}{\int_{a'}^{\infty} \frac{1}{\sqrt{\pi}} \exp(-\xi^2) d\xi} + \frac{\gamma_{*i}'}{B_{*i}\eta_0} - 1 \tag{17}$$

$$a' = B_{*i} / \gamma_{*i}' - 1/\eta_0, \ \eta_0 = 0.5, \ \alpha_* = 0.14, \ K = 0.008$$

$$B_{*i} = \xi_i B_{*0}$$

$$\xi_i = \frac{\gamma_{*ci}}{\gamma_{*ci0}}$$

where q_{sui} is the suspended volume from the bottom per unit area [m/s], and w_{fi} is the fall velocity of suspended sediment according to diameter [m/s].

The volumetric fraction of the bed material grain size is obtained from:

$$\delta \frac{\partial p_i}{\partial t} + p_i^* \frac{\partial \eta}{\partial t} + \frac{1}{1-\lambda}\left[\frac{1}{B} \frac{\partial (q_{Bi} B)}{\partial x} + q_{sui} - w_{fi} c_{bi} \right] = 0 \tag{18}$$

$$p_i^* = p_i; \ \partial\eta / \partial t \geq 0$$

$$p_i^* = p_{i0}; \ \partial\eta / \partial t < 0$$

where δ is the thickness of the exchange layer [m] and λ is the porosity of the bed material/void ratio [-], η is the river bed elevation [m], p_{io} is the volumetric fraction of bed material in suspension at the beginning of simulation [-], and p_i is the volumetric fraction of bed material in suspension at a given time step [-].

The time-dependent bottom profile change is obtained from the continuity of bed material transport:

$$\frac{\partial \eta}{\partial t} + \frac{1}{1-\lambda}\left[\frac{1}{B} \frac{\partial \sum_i (q_{Bi} B)}{\partial x} + \sum_i \left(q_{sui} - w_{fi} c_{bi} \right) \right] = 0 \tag{19}$$

2.4 Finite difference equation formulation

2.4.1 Flow equation

In finite difference form the flow equation, Equation (12) can be written as:

$$\left(\frac{Q^2}{2gB^2h^2}+H-\frac{\Delta x}{2}\frac{Q^2n^2}{B^2h^{10/3}}\right)_j=\left(\frac{Q^2}{2gB^2h^2}+H+\frac{\Delta x}{2}\frac{Q^2n^2}{B^2h^{10/3}}\right)_{j-1} \tag{20}$$

Shear velocity and bed shear are calculated as shown below:

$$u_*=\sqrt{ghi_e} \tag{21}$$

$$\gamma_{*i}=\frac{u_*^2}{sgd_i} \tag{22}$$

2.4.2 Diameter and profile change

Particle size change and profile change are calculated by changing Equations (18) and (19) in finite difference form, respectively:

$$\delta\frac{p_{ij}^{n+1}-p_{ij}^{n}}{\Delta t}=-p_{ij}^{*}\frac{\eta_j^{n+1}-\eta_j^{n}}{\Delta t}+\frac{1}{1-\lambda}\left[\frac{(Bq_{Bi})_{j-1}^{n}-(Bq_{Bi})_j^{n}}{\Delta B_j}-\left(q_{sui}-w_{fi}c_{bi}\right)_j^{n}\right] \tag{23}$$

$$\frac{\eta_j^{n+1}-\eta_j^{n}}{\Delta t}=\frac{1}{1-\lambda}\left[\frac{\left(B\sum_i q_{Bi}\right)_{j-1}^{n}-\left(B\sum_i q_{Bi}\right)_j^{n}}{\Delta B_j}-\sum_i\left(q_{sui}-w_{fi}c_{bi}\right)_j^{n}\right] \tag{24}$$

where n and $n+1$ are time step counters [-].

2.5 Sediment transport

Sediment transport in the channel is a function of two processes, deposition and degradation, operating simultaneously in the reach. Sediment yield concentration from the watershed reaching the subbasin stream at the beginning of the time step is compared with the transport capacity (T_c) of that stream segment. If the initial concentration of sediments reaching the stream segment is greater than the transport capacity of the stream segment deposition is the dominant process, otherwise degradation of the stream is the dominant process. The river profile is then updated at the end of the time step and the process continues again. From the experimental analysis of the river transport capacity, Bagnold (1977) established that the transport capacity of the river is a function of peak velocity in the channel; based on the work by Bagnold, the transport capacity (T_c) for this case is calculated as (Arnold, *et al.*, 1995).

$$T_c=aV_{pk}^{\ b} \tag{25}$$

$$V_{pk}=\frac{q_{pk}}{A_{ch}} \tag{26}$$

where A_{ch} is the cross-sectional area of flow in the channel [m^2], q_{pk} is the peak flow rate in the channel [m^3/s], T_c is the transport capacity [ton/m^3], V_{pk} is the peak channel flow velocity [m/s], and a and b are the channel coefficients.

The net amount of sediment deposited and eroded is calculated:

$$sed_{dep} = (C_{in} - T_c) \cdot V_{ch} \tag{27}$$

$$sed_{\deg} = (T_c - C_{in}) \cdot V_{ch} \cdot K_{ch} \cdot C_{ch} \tag{28}$$

where sed_{dep} is the amount of sediment deposited in the reach segment [tons], V_{ch} is the volume of water in the reach segment [m^3], sed_{deg} is the amount reentrained in the reach segment [tons], K_{ch} and C_{ch} are the channel coefficients [-] and C_{in} is initial concentration of the sediments reaching the stream segment [ton/m^3].

Once the amount of deposition and degradation has been calculated, the final amount of sediment in the reach and the amount of sediment transported out of the reach is determined:

$$sed_{ch} = sed_{ch,i} - sed_{dep} + sed_{\deg} \tag{29}$$

$$sed_{out} = sed_{ch} * \frac{V_{out}}{V_{ch}} \tag{30}$$

where sed_{ch} is the amount of suspended sediment in the reach [tons], $sed_{ch,i}$ is the amount of suspended sediment in the reach at the beginning of time period [tons], sed_{out} is the amount of sediment transported out of the reach [tons], V_{out} is the volume of outflow during the time step [m^3], and V_{ch} is the volume of water in the reach segment [m^3].

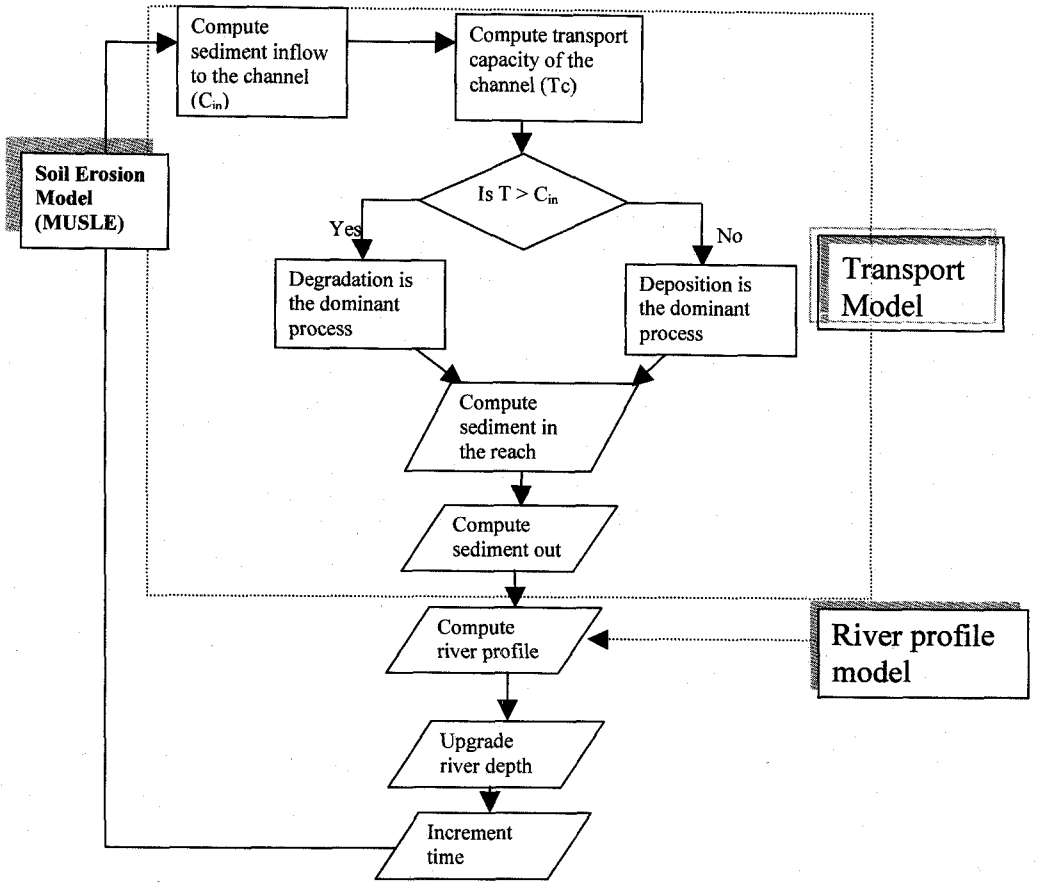

Figure 3. Flow Chart for the integrated Model.

3. Effect of land use change

In this part the effect of land use change to the sediment discharge to the coastal environment is analyzed. Land use data are compiled from remote sensed images for the years 1976, 1987, 1991 and 1997. There is no significant change in the land use between 1976 and 1987 and also between 1991 and 1997. Significant land use change can be observed between years 1976 and 1997. Hence, the land use data for the years 1976 and 1997 are used for analyzing the effect of land use change to sediment discharge.

In the MUSLE model the parameters which are function of land use are SCS curve number (CN), land cover factor (C) and land management factor (P). CN is an index developed by the SCS to represent the potential for storm water runoff within a drainage area. In calculating the quantity of runoff from a drainage basin, the curve number is used to determine the amount of the precipitation excess that results from a rainfall event over the basin.

3.1 Curve number (CN)

Because CN is a function of the soil and land use within the river basin, its estimation requires mapping of the soil and land use within the basin boundaries, and specification of unique soil types and unique land use categories. The important physical parameter for the soil is hydrologic soil group, which is defined as a group of soils having similar runoff potential under similar storm and cover conditions. SCS classifies the soils into four hydrologic groups. In this analysis, the FAO soil data is used to estimate the percentage of each soil unit belonging to the four hydrologic soils groups. Since the CN is the function of both soil and land use cover, the soils and land cover shape files are merged using GIS.

3.2 Land cover (C) and land management (P) factors

The values of C and P factors are related to the land use identified by land cover type. Land cover originally categorized by the USGS global ecosystems legend is reclassified into 13 types according to their similarity (Table 1). Referring to Wischmeir and Smith, (1965), an average value of the C factor is given to each land cover type in the Table. The P factor accounts for control practices that reduce the erosion potential of the runoff by their influence on drainage patterns, runoff concentration, runoff velocity and hydraulic forces exerted by runoff on soil (Renard *et al.*, 1997).

Table 1. Land cover classification and land cover (C) and land management (P) factors.

Land cover	C factor	P factor
Urban area	0.1	1.0
Bare land	0.35	1.0
Dense forest	0.001	1.0
Sparse forest	0.01	1.0
Mixed forest and cropland	0.1	0.8
Cropland	0.5	0.5
Paddy field	0.1	0.5
Dense grassland	0.08	1.0
Sparse grassland	0.2	0.1
Mixed grassland and cropland	0.25	0.8
Wetland	0.05	1.0
Water body	0.01	1.0
Permanent ice and snow	0.001	1.0

Using the land use cover for the years 1976 and 1997, the sediment yield and hence sediment discharge to the river mouth is calculated for each land cover and the comparison of the results were made.

4. Climate change

The climate change scenarios are simulated using General Circulation Models (GCMs). As the evaluation of Takahashi et al. (2001), HadCM2 model developed at the Hadley Centre gives comparatively high accuracy. GCMs are good at long term predictions of climate variables but poor at weather predictions. From the mean daily rainfall data for the month for the period 2040-2050 generated using HadCM2 model, the daily rainfall is generated using stochastic weather data

generator model, WXGEN (Sharpley and Williams, 1990). The rainfall generator model, WXGEN, use the first order Markov chain model developed by Nicks (1974). With the first order Markov chain, the probability of rain on any given day is conditioned by the wet or dry status of the previous day. A wet day is defined as a day with rainfall greater than 0.1mm. Given the wet-dry probabilities, the model stochastically determines the occurrence of rainfall in a particular day. For this study, the amount of rainfall in a wet day is calculated using exponential distribution.

$$R_{day} = \mu_{month}\left(-\ln(rnd_1)\right)^{rexp} \tag{31}$$

where R_{day} is the amount of rainfall on a given day [mm], μ_{month} is the daily mean monthly rainfall [mm], rnd_1 is the random number between 0.0 and 1.0, and *rexp* is a dimensionless constant with value between 1.0 and 2.0.

From the generated amount of daily rainfall for the period 2040-2050, amount of sediment discharge to the river mouth is calculated and the results were compared with the 1990-2000 results.

5. Results and discussion

5.1 Total sediment discharge to coastal environment

As shown in Figure 1, the river basin is divided into the total number of 19 subbasins using GIS software from Digital Elevation Model (DEM). Figure 4 shows the comparison between the observed and the simulated flow. Simulated flow values are in close agreement with the observed values. However, in some months the difference between observed and simulated values is relatively high. Figure 5 shows the scatter plot and linear regression line between the observed and simulated stream flow values with the correlation coefficient (R^2) of 0.81. Simulated results for subbasins 17, 18 and 19 are as shown in Figure 6. Sediment yield is computed for each subbasin for each time step. Since the routing mechanism starts from the most upstream subbbasins, for each time step, sediments from the upstream subbasins are accumulated to the sediment yield of the downstream subbasins as a result subbasin 19 has the highest sediment discharge because it is the most downstream subbasin and it accumulates all the sediments from upstream subbasins. Figure 7 shows the relationship between sediment discharge and the river flow; generally there is strong relationship between the two, the periods with high sediment discharge corresponds to high river flow and periods with low sediments discharge correspond with low river flow periods; in particular, the period between 1992 and 1997 has low sediment discharge at the river mouth and the corresponding flows for this period is also low. The scatter plot between the observed flow and the sediment discharge at the river mouth is shown in Figure 8, and the correlation coefficient (R^2) between the two is 0.67. Figure 9 shows measured sediments data at the river mouth; annual sediment inflow from the river basin to the river mouth is calculated as a total of deposited sediments and dredged sediments for each year. The comparison between the simulated sediments and the measured sediments at the river mouth for the period between 1990 and 2000 are as shown in Figure 10. Since the only available measured data is yearly data, the comparison was done only on annual basis. It can be observed that there is a good agreement between the observed and measured sediments data. For the sediment routing mechanism used in this study, it was impossible to separate between the washload and the bed load. However, the total sediments discharge to the river mouth includes both washload and bed load.

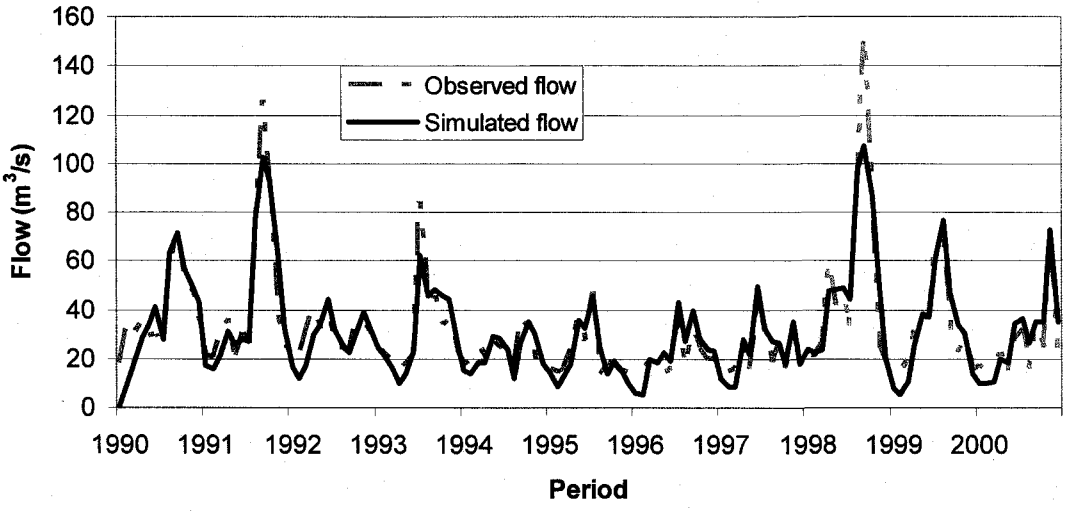

Figure 4. Comparison between observed and simulated flow.

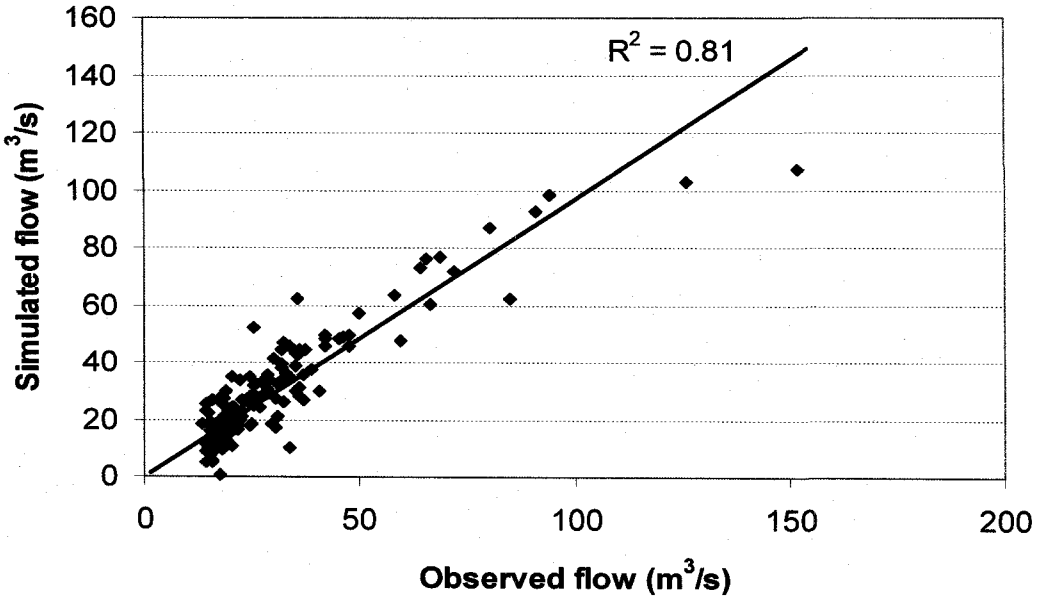

Figure 5. Scatter plot and linear regression line between the observed and simulated stream flow values.

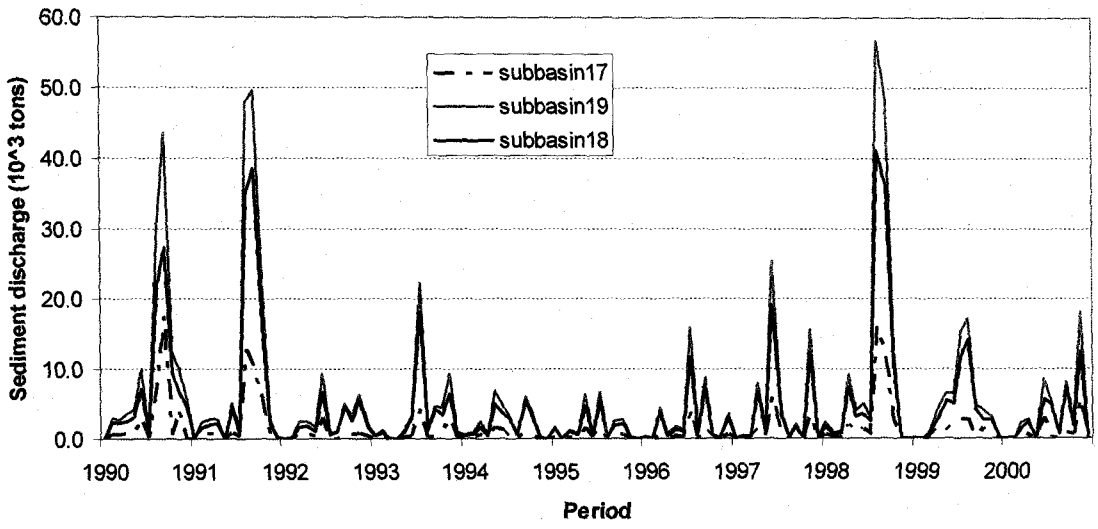

Figure 6. Monthly sediment discharges at the outlets of subbasins 17, 18 and 19.

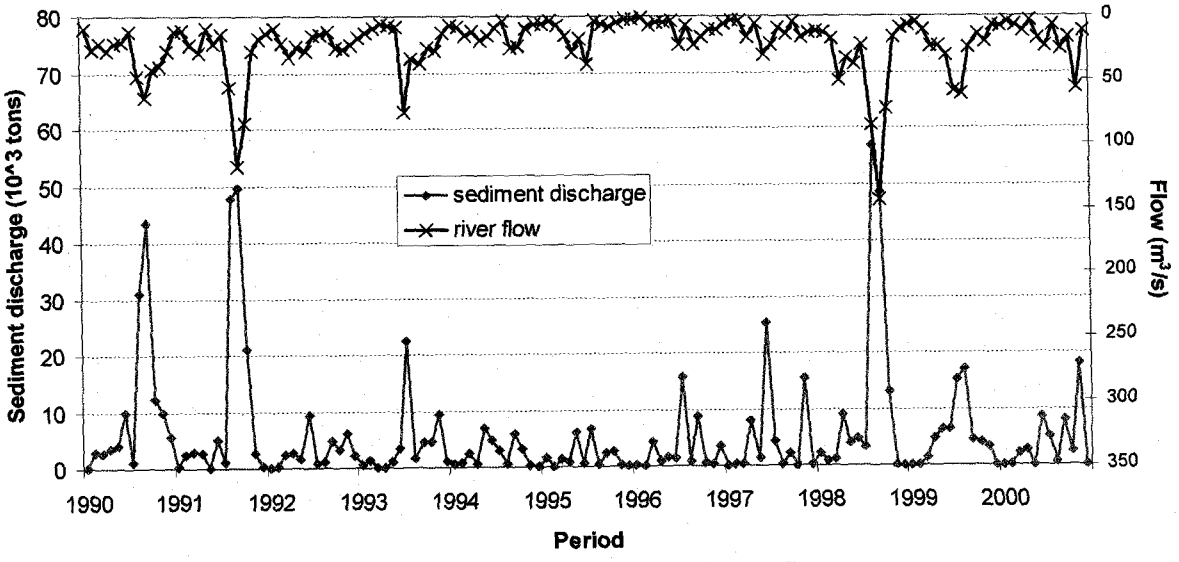

Figure 7. Comparison between sediment discharge and river flow.

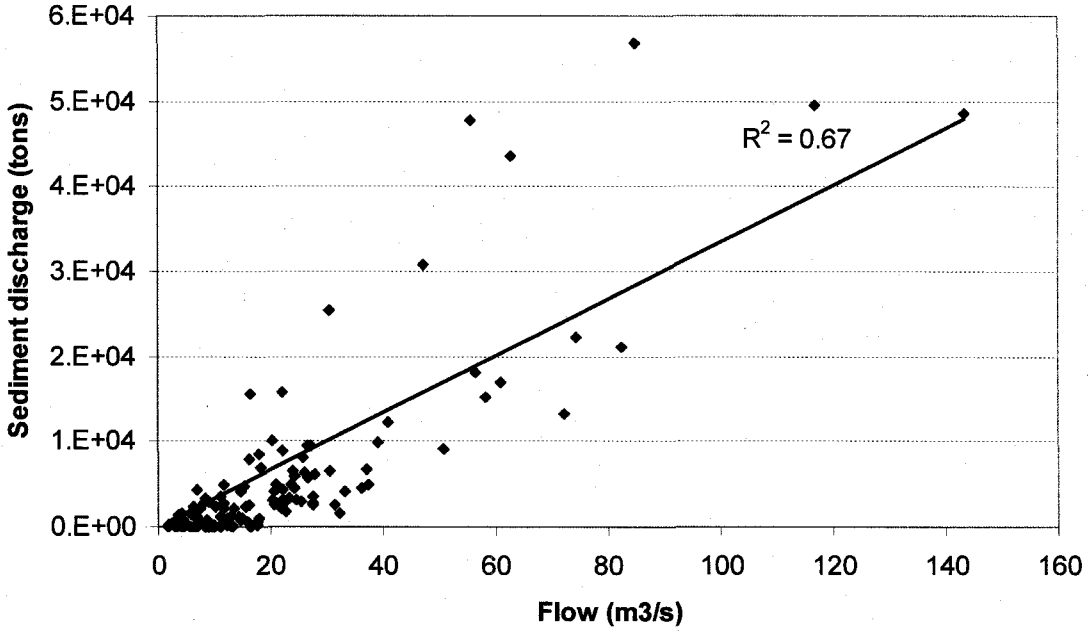

Figure 8. Scatter plot between stream flow and the sediment discharge.

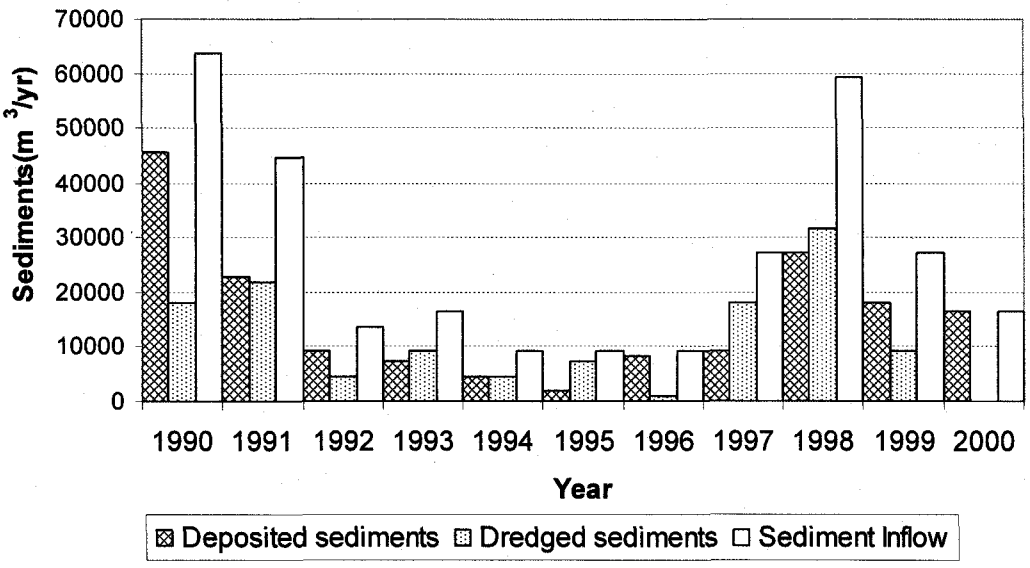

Figure 9. Measured sediments data at the river mouth.

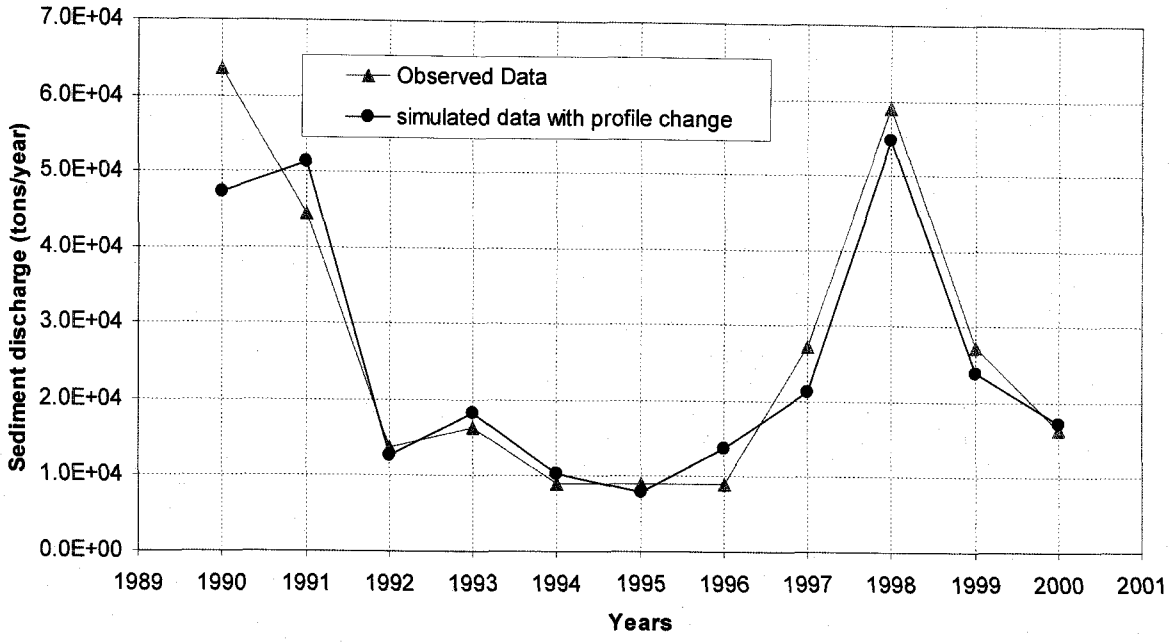

Figure 10. Observed and simulated sediments for the period 1990-2000 at Iizumi.

5.2 Effect of land use change

Figure 12 shows the comparison of the amount of sediment discharge to the river mouth using the land cover/land use for the years 1976 and 1997. From the graph, it can be seen that the sediment discharge is higher using the land cover for the year 1997 as compared to 1976. This can be attributed to increase in agricultural areas and residential areas within this period of 21 years as shown in Figure 11.

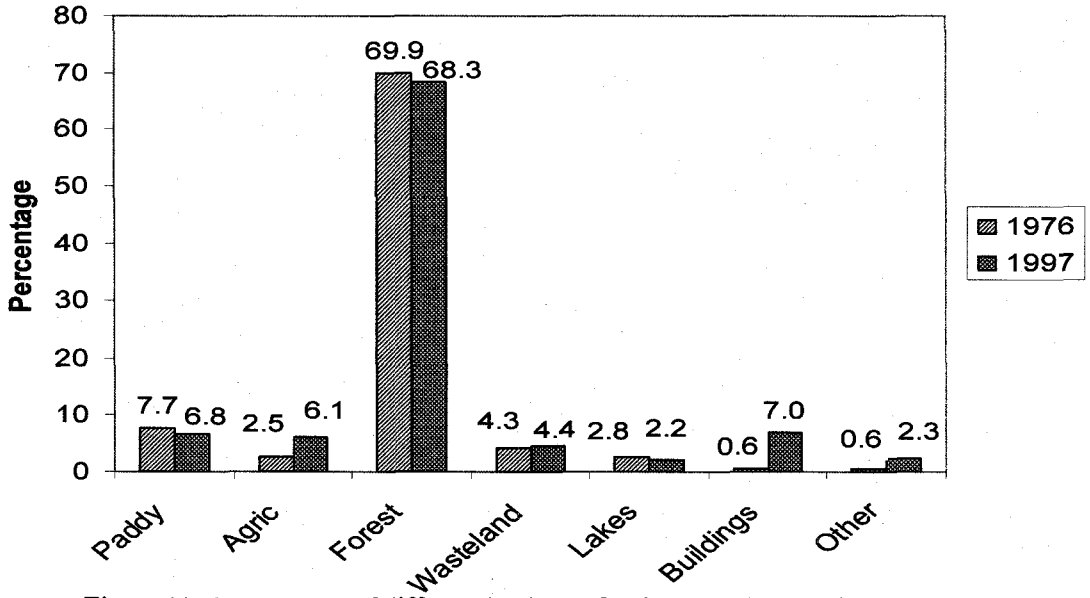

Figure 11. Percentages of different land uses for the years 1976 and 1997.

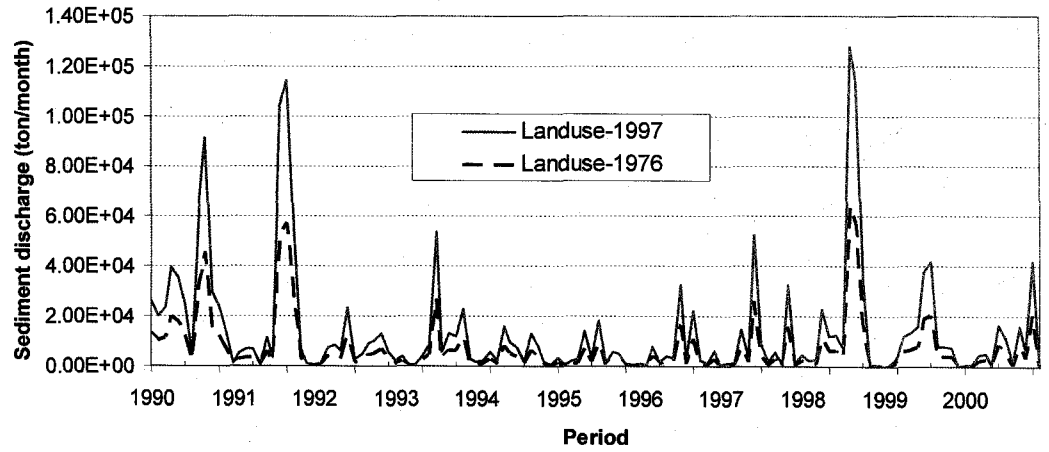

Figure 12. Comparison of sediment discharge at the river mouth using the land cover for the year 1976 and 1997.

5.3 Effect of climate change

Figure 13 shows the total annual sediment discharge for the periods 1990-2000 and 2040-2050 and Figure 14 shows the simulated mean monthly sediments discharge at the river mouth for the present and future climate scenarios. From both figures, it can be seen that there is no clear trend for the sediment discharge at the river mouth that can be deduced despite the fact that there are some years e.g. 2050 with highest total sediment discharge. Figure 15 shows simulated mean monthly runoff for the period 1990–2000 and 2040–2050. From the graph, it can be seen that the future

simulated runoff is less compared with the future scenario. This decrease in runoff can be attributed to decrease in the amount of rainfall for the future scenario as compared the current period.

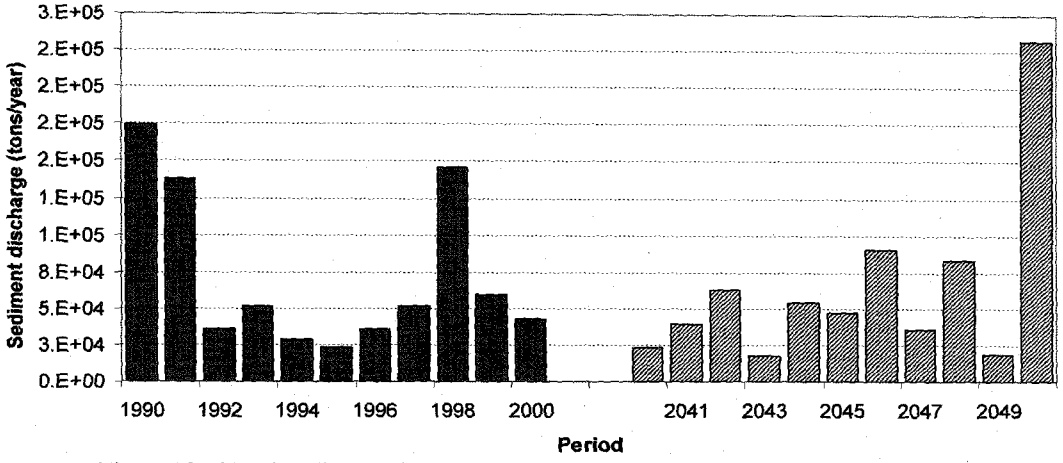

Figure13. Total sediment discharges for the periods 1990-2000 and 2040-2050.

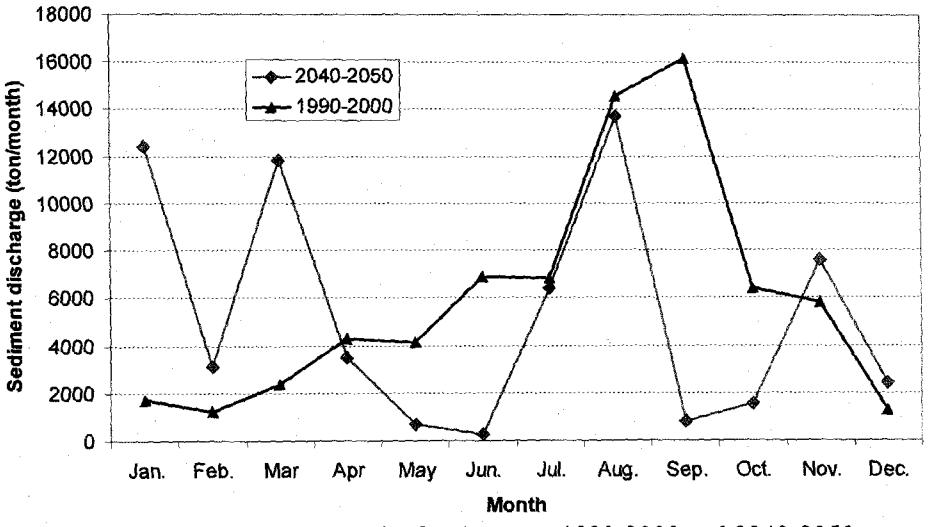

Figure 14. Simulation results for the years 1990-2000 and 2040-2050.

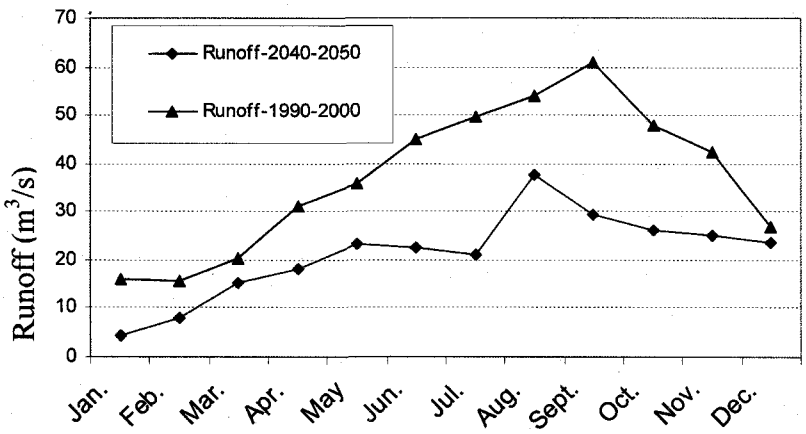

Figure 15. Comparison between current precipitation and simulated future precipitation (2040-2050).

5.4 Sensitivity of the parameters

Sensitivity analysis was done for two parameters of the model, CN and land cover factor (C). The values of the parameters were increased by 5% and 10% and the corresponding effect in the sediment yield was analyzed. The results of this analysis are shown in Figures 16 and 17. Increasing the curve number factor by 10% resulted in the increase in the annual sediment yield by around 75%, while increasing the land cover factor by 10% resulted in the sediment yield increase by 23%. From these results, it can be observed that CN factor is more sensitive parameter and therefore it has to be determined with the greater accuracy.

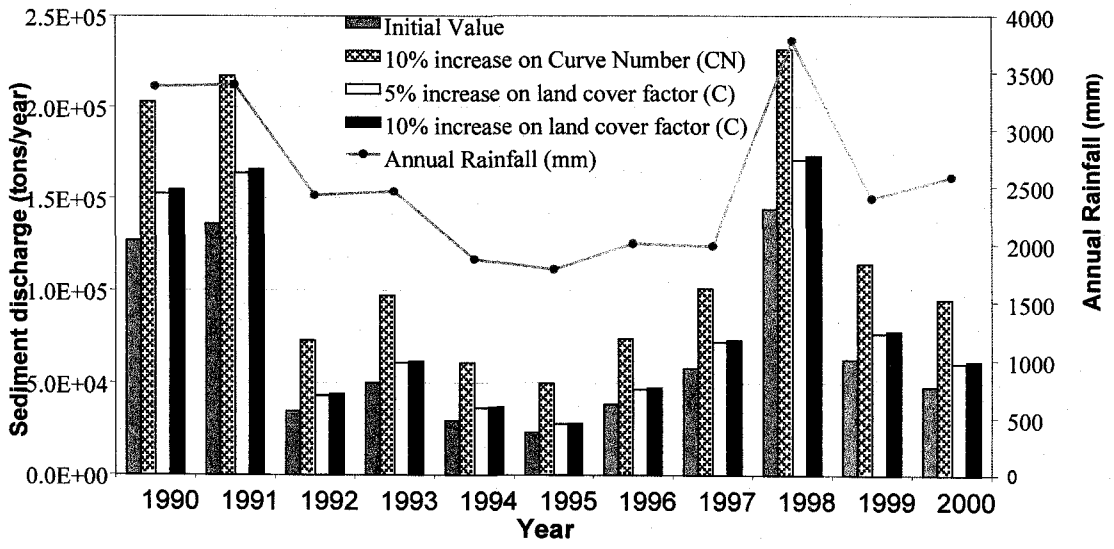

Figure 16. Effect of changing land cover factor (C) and curve number (CN) on the sediment. yield for subbasin 19.

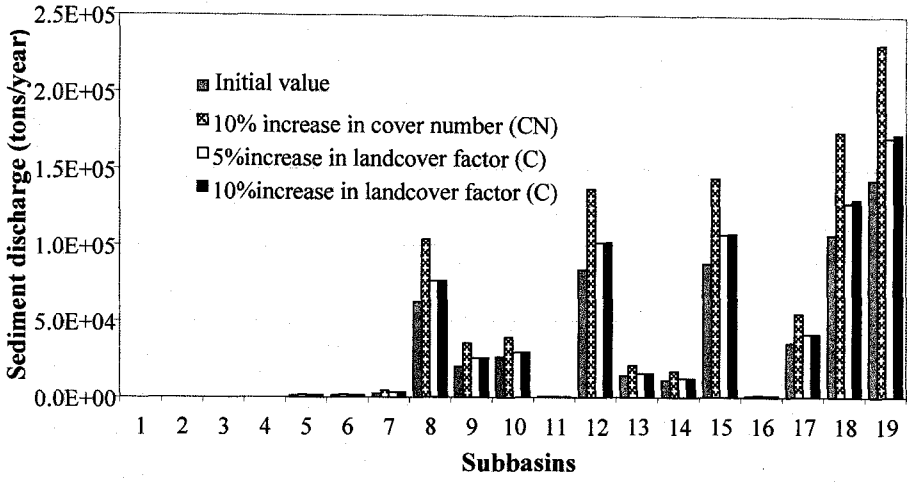

Figure 17. Effect of change in land cover factor (C) and curve number (CN) on the sediment yield for the year 1998 on different subbasins.

6. Conclusion

Sediment discharge from the river basin to the coastal environment is estimated in this study. The comparison between the observed and simulated results shows a reasonable good fit between the two. From the analysis of the effects of land use change, in which the land use data for the year 1976 and 1997 were used, it is observed that within the period of 21 years sediment discharge to the coastal environment increased. This can be attributed to decrease in forest cover from 69.9% in year 1976 to 68.3% in year 1997; increase in agricultural areas from 2.5% to 6.1% and also increase in residential areas from 0.6% to 7.0%. Analysis of future climate scenarios shows the high total sediment discharge for the year 2050, however for the rest of the years there is no clear trend which can be observed between the present and future climate scenarios. The average annual sediment discharge for the present period, 1990-2000 is about 7.88×10^5 ton/year; and for the future climate scenario, 2040-2050, the average sediment discharge to the coastal environment is about 7.07×10^5 ton/year. The decrease in sediment discharge to the coastal environment for the future climate scenario is probably due to decrease in the amount of precipitation which has resulted in low runoff. However, in the calculation of future sediment discharge to the coastal environment, the current land cover is used; no attempt is done to predict future land cover.

Acknowledgements

This study was supported by JSPS Grants-in-Aid for Scientific Research (B-15404016) and by JSPS AA Scientific Platform Program (coordinator, Tomoya Shibayama).

References

Arnold, J.G, Williams, J.R and Maidment, D.R. (1995): Continuous water and sediment routing model for large basins. *Journal of Hydraulic Engineering, ASCE, 121(2), 170-183*

Bagnold, R.A. (1977): Bed Load transport by natural rivers. *Water Resources Research, Vol. 13(2), 303-312*

Foster, G.R. (1982): Modelling the erosion processes. In: C.T. Haan (Editor), Hydrologic Modelling of Small Watersheds. *ASAE Monograph, pp. 297-380. In* Present and prospective technology for predicting sediment yield and sources: *Proceedings of the sediment yield workshop,* USDA Sedimentation Lab., Oxford, MS, November 28-30, 1972. ARS-S-40. p.244-252.

Govindaraju, R. S. and Kavvas, M. L. (1992): Characterization of the rill geometry over straight Hillslopes through spatial scales. *J. Hydro.*, Amsterdam, 130, 339–365.

Itakura, T. and Kishi, T. (1980): Open channel flow with suspended sediments. *Proc. of ASCE, HY8,* pp.1325-1343.

Lu, H., Gallant, J., Prosser, I.P., Moran, C. and Priestley, G. (2001): Prediction of Sheet and Rill Erosion over the Australian Continent, Incorporating Monthly Soil Loss Distribution. *Technical Report 13/01, CSIRO Land and Water, Canberra, Australia.*

Moore, I.D. and G.J. Burch. (1986): Modeling erosion and deposition: Topographic effects. *American society of agricultural engineers 000-2351:1624-1640.*

Neitsch, S.L, Arnold, J.G., Kiniry, J.R., Williams, J.R. and King, K.W. (2002): Soil and Assessment Tool (SWAT) theoretical documentation, version 2000, 506pp.

Nicks, A.D. (1974): Stochastic generation of the occurrence, pattern, and location of maximum amount of daily rainfall, pp. 154-171. *In Proc. Symp. Statistical Hydrology, Aug.-Sept.1971, Tucson, AZ, U.S. Department of Agriculture, Misc. Publ. No.1275*

Renard, K. G. et al. (1997): Predicting soil erosion by water: A guide to conservation planning with the Revised Universal Soil Loss Equation (RUSLE), US Department of Agriculture, Agriculture Handbook No. 703, 404pp.

Sharpley, A.N. and Williams, J.R. (1990): EPIC-Erosion/Productivity Impact Calculator: *USDA Technical Bulletin 1768:235pp.*

Soil Conservation Service (SCS) (1972): National Engineering Handbook, Section 4: Hydrology, US Department of Agriculture, USA.

Tayfur, G. and Singh, V.P. (2004): Numerical model for sediment transport over nonplanar, nonhomogeneous surfaces. *Journal of Hydrologic Engineering, ASCE, Vol.9, No.1 (2004) 35-41*

Tuan, L.T. and Shibayama, T. (2003): Application of GIS to evaluate long-term variation of sediment discharge to coastal environment. *Coastal Engineering Journal, Vol.45, No.2 (2003) 275-293*

Williams, J.R. (1975): Sediment-yield prediction with universal equation using runoff energy factor.

Wischmeir, W.H. and Smith, D.D. (1965): Predicting rainfall-erosion losses from cropland east of the Rocky Mountains. *Guide for Selection of Practices for Soil and Water Conservation. Agricultural Handbook* No. 282. USDA: Washington, DC.

Woolhiser, D. A., Smith, R. E. and Goodrich, D. C. (1990): KINEROS, A kinematic runoff and erosion model: *Documentation and user manual. ASR-77, U.S. Department of Agriculture, Washington, D. C., 130pp.*

Yang, D., Kanae, S., Oki, T., Koike, T. and Musiake, K. (2003): Global potential soil erosion with reference to land use and climate changes. *Wiley Interscience, Hydrological Process. 17, 2913-2928 (2003)*